Hydraulic Autonomous Soft Robotic Fish for 3D Swimming

Robert K. Katzschmann, Andrew D. Marchese and Daniela Rus

Abstract This work presents an autonomous soft-bodied robotic fish that is hydraulically actuated and capable of sustained swimming in three dimensions. The design of a fish-like soft body has been extended to deform under hydraulic instead of pneumatic power. Moreover, a new closed-circuit drive system that uses water as a transmission fluid is used to actuate the soft body. Circulation of water through internal body channels provides control over the fish's caudal fin propulsion and yaw motion. A new fabrication technique for the soft body is described, which allows for arbitrary internal fluidic channels, enabling a wide-range of continuous body deformations. Furthermore, dynamic diving capabilities are introduced through pectoral fins as dive planes. These innovations enable prolonged fish-like locomotion in three dimensions.

Keywords Soft robotics · Robotic fish · Hydraulic actuation · Underwater locomotion · Lost-wax silicone casting · Soft actuator fabrication · Fluidic elastomer actuator

This work was done in the Distributed Robotics Laboratory within CSAIL at MIT with support from the National Science Foundation, grant numbers NSF 1117178, NSF EAGER 1133224, NSF IIS1226883 and NSF CCF1138967, and National Science Foundation Graduate Research Fellowship Program, primary award number 1122374. We are grateful for this support. The authors declare no competing financial interests.

R.K. Katzschmann (✉) · A.D. Marchese · D. Rus
Computer Science and Artificial Intelligence Laboratory, Massachusetts Institute of Technology, 32 Vassar Street, 32-376, Cambridge, MA 02139, USA
e-mail: rkk@csail.mit.edu
URL: http://www.csail.mit.edu

A.D. Marchese
e-mail: andy@csail.mit.edu

D. Rus
e-mail: rus@csail.mit.edu

M.A. Hsieh et al. (eds.), *Experimental Robotics*, Springer Tracts in Advanced Robotics 109, DOI 10.1007/978-3-319-23778-7_27

1 Introduction

Many natural system have body compliance as an integral functional feature. Compliant bodies easily adapt to changes in the environment and compensate for its uncertainties. This adaptability reduces the complexity in modeling, planning, and control. During a collision, a compliant body can deform and absorb energy [1], which allows for safer interaction between humans and robots. The aim is to exploit the principle of body compliance and design softness into robots.

In this work, an approach to create and control an autonomous soft-bodied system for prolonged motion underwater is presented. It is demonstrated that a soft actuator can be used untethered for controlled continuous propulsive locomotion in a fluidic medium. This allows for use in underwater inspection tasks of complex shaped environments where body compliance and adaptability is key in navigating through branched structures like pipe systems. It also has the potential to be used for close studies of fish schools. Deploying a soft robotic fish which mimics the locomotion of a biological fish will more likely be accepted to swim along fish schools without disrupting their natural behavior.

1.1 Overview

This paper presents a hydraulically actuated soft-bodied robotic fish that can swim for long durations of time and move in three dimensions to control depth and planar trajectories. In order to enable these new capabilities, innovations in the design, fabrication, and control of the biologically inspired soft body and its drive system are shown. The soft body, fundamentally composed of distributed fluidic elastomer actuators [2–4], provides continuous undulatory motion as in [5], but is using hydraulic instead of pneumatic actuation. This modified body is fabricated through an innovative wax molding and casting process. The propulsive and steering actuation of the deformable body is driven by a novel closed-circulation water system. An open-loop controller for this new drive system is described and the integration into a closed-loop controller using an inertial measurement unit is laid out. Lastly, the entire system is experimentally validated by demonstrating forward swimming and yaw motions using the soft tail, and pitch control using dive planes.

1.2 Previous Work

Previous work has shown many approaches to building fish-like robots. Traditionally, robotic fish were hard, meaning they have bodies composed of rigid links and a finite number of joints [6–10]. A motor-less and gear-less approach was to use shape memory alloys to build robotic fish with a hard skeleton shell but with a deformable backbone for fish tail actuation [11].

Alternatively, soft-bodied robots have continuously deformable backbones and theoretically infinite degrees of freedom [12]. There are several examples of soft-bodied fish-like robots that use centralized actuation. A soft-bodied octopus-like arm developed by Laschi et al. demonstrated shortening, elongation and bending [13]. The robot fish FILOSE [14, 15] has a compliant posterior and demonstrated fishlike locomotion. Valdivia y Alvarado and Youcef-Toumi used a soft and compliant body in the design of a robotic fish to mimic the forward swimming kinematics of a real fish [16]. All three of these systems are cable-driven and actuated with an onboard servomotor, but require an external power supply and lack autonomy. Long et al. have developed a flexible biomimetic vertebral column used to propel an autonomous surface-swimming robot [17, 18]. Again, a single servomotor is used to actuate the compliant spine. It is an autonomous surface swimming system with only the posterior part of the tail being flexible. The above-mentioned compliant-bodied robotic fish operate on the principle of a passive, flexible mechanism driven by a traditional electromechanical actuator. They are primarily designed to study the hydrodynamics of the flexible body.

There are also examples of compliant active-bodied robots that achieve fish-like locomotion using distributed actuation. Shen et al. have used an oscillating strip of ionic polymer-metal composite as the posterior trunk of a dolphin-like robot [19]. Suzumori et al. developed a soft-bodied manta using pneumatic actuation [20]. Both systems are free swimming robots, but are also limited by an external tether.

The Airacuda fish developed by Festo [21] uses tube-shaped pneumatic muscles to actuate a flexible posterior body. The posterior body is composed of a rigid plastic skeleton covered by flexible skin and has the two actuating muscles at its center axis. In comparison, the posterior body presented in this work is composed almost entirely of soft rubber with many fluidic elastomer actuators embedded along both sides. The fluidic and electronic components of Airacuda are located in the fishs rigid anterior. The Airacuda uses its pneumatic actuation system not only for forward swimming and turning motions, but also for static diving, whereas the hydraulic system presented in this work uses dive planes for dynamic diving.

The previous work by Marchese et al. [5] has a fluidic actuation system that is embedded within the compliant and flexible body. This completely self-contained and autonomous system is capable of rapidly achieving continuum-body motion, emulating forward swimming and planar escape maneuvers of biological fish.

1.3 Extensions of Previous Work

This work extends in several ways the autonomous soft-bodied fish by Marchese et al. [5]. In this previous work, it was demonstrated that soft robots can be both self-contained and capable of rapid body motion. However, there are several prohibitive shortcomings of this previous implementation. (1) The fish used an open-circulation pneumatic actuation system that made prolonged operation difficult; after energy was delivered to the distributed body actuators, it was exhausted to the environment. This limitation is addressed in this paper by designing a closed-circulation drive system. (2) The previous implementation was pneumatically actuated without using an air bladder. The center of buoyancy was therefore uncontrollably changing throughout the actuation cycle. Designing the system to use water as a transmission fluid and being neutrally buoyant addresses this use. (3) The previous implementation was constrained to move on a pre-defined trajectory in two dimensions, which is addressed by introducing dive planes to allow for dynamic diving.

1.4 Major Contributions

This work differs from previous work in that distributed hydraulic actuation, a new drive system for this kind of actuation, and new fabrication techniques to cast the distributed fluid elastomer actuator are used. Specifically, the following contributions are made:

1. Design of a water-driven soft-bodied actuator and a closed-circulation hydraulic drive system;
2. Fabrication technique for a soft-bodied actuator that allows arbitrarily formed fluidic channels, enabling a wide-range of continuous bending profiles;
3. Biologically inspired fish-like gait and dynamic diving, enabling forward-swimming in 3D.

2 Technical Approach

The technical approach to develop an autonomously propulsing soft robotic fish includes the mechanical design of individual functional units, a new fabrication technique for fluidic elastomer actuators, and a control approach for the locomotion and steering of the fish.

2.1 Mechanical Design

The robotic fish consists of three major functional components. These are:

1. the fish's soft tail for forward propulsion and yaw motions,
2. a waterproof gear pump unit as actuation source for the tail, and
3. a pair of dive planes actuated by a waterproof servo to enable pitch control.

Furthermore, a dorsal and a ventral fin were added to protect the fish against rolling. The control electronics are placed in a watertight nose compartment. Figure 1 shows the robotic fish with all its major components.

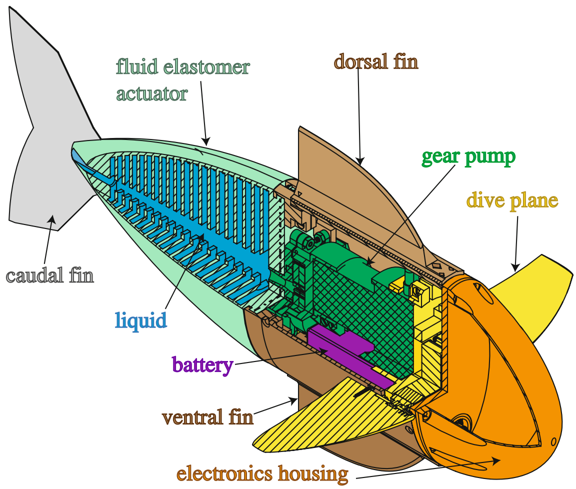

Fig. 1 Isometric cut of fish assembly

2.2 Fish Tail

The soft fish tail shown in Fig. 2 belongs to the group of fluidic elastomer actuators [2, 3]. The design mimics the rear portion of a fish, encompassing the posterior peduncle and the caudal fin. This tail can continuously bend along its vertical center constraint layer by fluidic actuation of two lateral cavity structures on each side. The

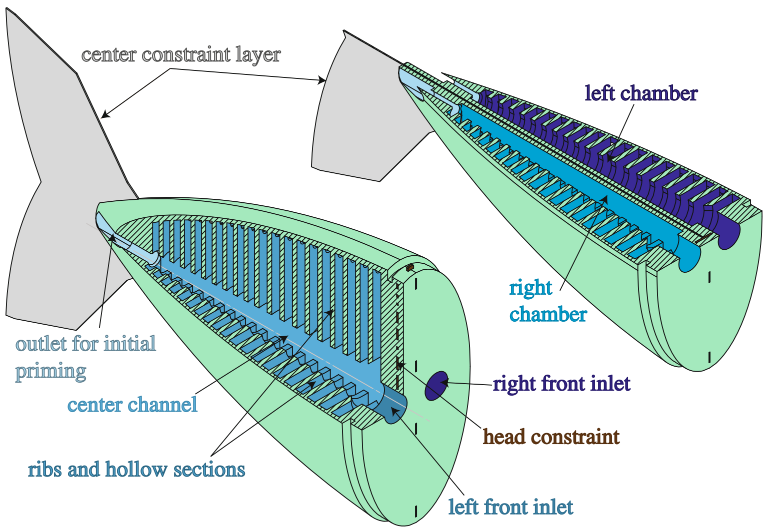

Fig. 2 Fish's soft tail as a fluidic elastomer actuator consisting of two fluidic chambers, visualized with two different cut views

inextensible and stiffer center constraint layer splits the tail evenly along a vertical plane. An actuator consists of evenly spaced ribs with hollow sections in between, connected by a center channel and accessible by a front inlet. The rib structure allows for expansion or contraction of the thin exterior skin under positive or negative fluidic pressure, respectively. The sum of these expanding or contracting motions leads to bending of the inextensible center constraint layer.

2.3 Fluidic Actuation Source

Previous approaches with pneumatic actuation using compressed gas cartridges as an energy source allowed for fast propulsion, but it was depleted after about 50 actuations [5]. Only a rather small compressed gas cartridge fits into the self-contained fish robot. The energy to weight ratio of a compressed gas cartridge is lower than modern batteries. In order to deflate an actuator, all the gas inside it is exhausted to the environment without reusing any of its kinetic energy. Furthermore, constantly releasing gas causes non-neglible changes in the overall buoyancy of the robotic fish, which either requires compensation through an air bladder or choosing a different actuation approach. Alternately transporting fluid from one chamber to the other does not require a storage unit in between, and the fluid does not need to be exhausted in order to deflate the actuator. This motivated a closed circulation actuation approach using an incompressible fluid like water and a gear pump to move it back and forth. The gear pump including its actuating DC motor are shown in Part b of Fig. 3.

The desired flapping frequency and curvature of the soft tail are determined based on previous studies on self-propelling foils driven by an external robotic actuator [22, 23]. The frequency and amplitude is applied onto a soft fish tail using a hydraulic

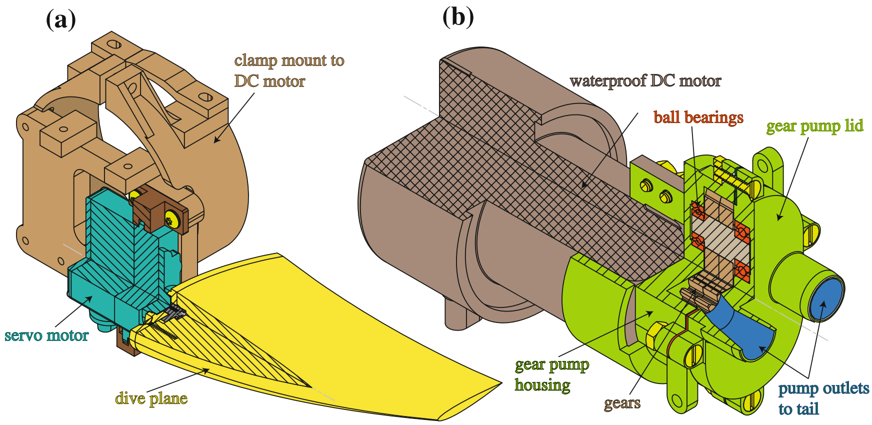

Fig. 3 **a** Dive plane attached to waterproof servo and clamp mount, and **b** gear pump with dc motor

cylinder pump. The measurements on the displaced volume and maximum pressures of the fish tail prototype combined with the desired flapping frequency result in the desired volumetric flow rate. Based on those results, a gear pump and its attached waterproof DC motor are designed and specified. The volumetric displacement per shaft revolution of an external gear pump is estimated with $Q = \frac{\pi}{4}\,(D^2 - d^2)\,w$, where w is the gear width, D is the gear's outer diameter, and d is the gear's inner diameter [24].

2.4 Dive Planes for Pitch Control

In order to allow for pitch motion and therefore dynamic diving, a pair of servo actuated dive planes are designed and added to the design at a place, where a fish's pectoral fins are usually located. Pectoral fins are responsible for the creation of a dynamic lifting forces to allow for depth control. One dive plane including its clamp mount to the back of the DC motor is shown in Part a of Fig. 3. The dive plane profile is designed using a loft limited by two symmetric air foil wing sections. A National Advisory Committee for Aeronautics (NACA) 0013 profile with a cord length of 0.06 m and a NACA 0010 profile with a cord length of 0.025 m was used. The cord length was determined by setting it to approximately 13 % of the entire length of the body of the fish. The thickness is defined by the size of the lever arm of the waterproof servo, which in return defines the size of the mounting plate needed. A symmetric profile is chosen so that no lift is produced when held in a horizontal position.

2.5 Fish Tail Fabrication

The actuated cavities of the fish tail are achieved by lost-wax casting. The fabrication process is depicted in Fig. 4.

In step (A), the rubber mold is poured and cured inside an assembly consisting of an outer mold with lid and a model for the core inside of it. In preparation for step (B), the lid and the model core are removed and the rubber mold is left inside the outer mold. The rubber mold receives a small carbon fiber tube as an inlay in its center cavity. This ensures that the wax core does not break when being removed from the rubber mold. Mold release spray is applied to the silicone rubber mold to ease the wax core removal process. The wax is heated up until it becomes fully liquefied. The assembly of rubber mold and outer mold is heated up for a few minutes to the same temperature as the wax. Using a syringe, the liquid wax is injected into the assembly. Within a few minutes, the injected wax will start to solidify and significantly shrink in volume; this is counteracted by injecting more hot wax into the solidifying wax core during the cool down. In step (B), the wax core is first allowed to completely

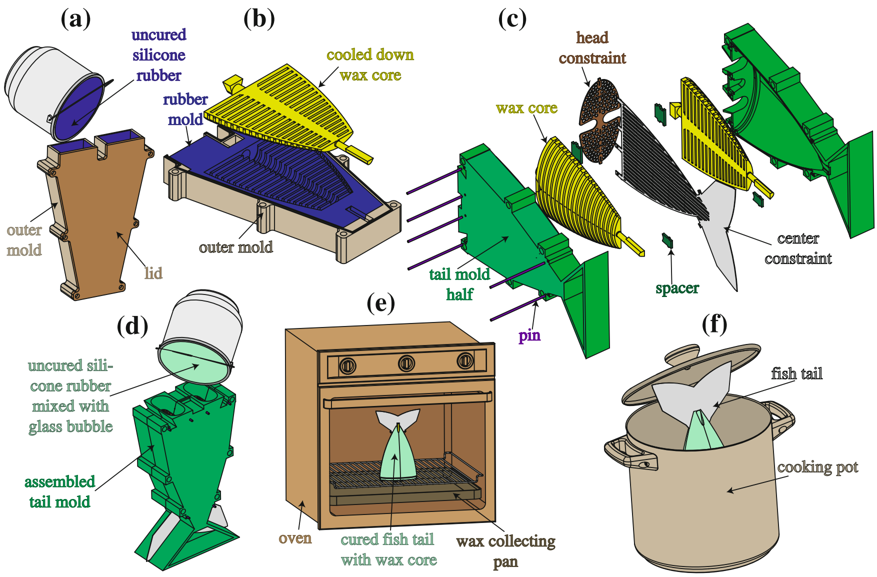

Fig. 4 Fish tail fabrication process: **a** Pour and cure a rubber mold, **b** pour wax cores, **c** combine head constraint, center constraint and wax cores with tail mold halves, **d** pour rubber mixed with glass bubbles into assembled tail mold, **e** using an oven melt out wax core from the cured fish tail, and **f** cook out remaining wax to create desired actuator cavities

cool down, then it is released from the mold. In step (C), a head constraint, a center constraint, and two wax cores are assembled together inside the tail mold halves using spacers, positioning pins and screws. In step (D), a mix of silicone rubber with glass bubbles is poured into the tail assembly and allowed to cure. In step (E), most of the wax core is melted out by placing the fish tail in an upright position into an oven. Finally, in step (F) the remaining wax residues are cooked out in a boiling water bath.

2.6 Control

The motion control of the robotic fish is mainly determined by the propulsive forward swimming motion of the soft tail. Yaw control is achieved through keeping, on average, more fluidic volume in one fish half than the other. Pitch control is done through adjusting the attack angle of the dive planes. Both yaw and pitch control effort depend on the forward swimming speed by the tail. An on-board 9 degrees of freedom inertial measurement unit provides absolute attitude measurements, which will be used in a future version of the fish for closed-loop attitude control.

2.6.1 Forward Swimming

Controlling the speed of the gear pump determines the volumetric flow from one side of the fin to the other. Alternating actuation at approximately 1 Hz results in a flapping motion of the posterior peduncle and phase-shifted flapping of the caudal fin. The voltage profile of the motor is shaped with an alternating trapezoidal profile to avoid impulsive switching, high peak currents, and high angular momentum around the roll axis. To adjust the forward swimming speed, the frequency and motor velocity are controlled.

2.6.2 Yaw Control

Controlling the heading requires that the fish tail has an adjustable average offset from the neutral tail position. This can be achieved by adjusting the alternating actuation so that on average more fluidic volume flows into one fish half than the other. This can be done by (a) adjusting the amplitude ratio between the positive and negative actuation trapezoid while keeping the time duration of both trapezoids the same, or (b) adjusting the ratio of time duration of both trapezoids so that one half is filled up longer than the other. The latter approach was chosen for the fish presented in this work. A combination of both methods is also possible.

2.6.3 Pitch Control

Controlling the pitch of the fish is achieved through adjusting the attack angle of the dive planes in a range of $-\frac{\pi}{4}$ to $\frac{\pi}{4}$ rad. The forward swimming speed directly determines how fast the pitch of the fish is changed and can be maintained.

3 Results

The implemented fabrication process for the wax is depicted in Fig. 5, showing each major step from silicone rubber mold creation to de-molding of the wax core. The outer mold, the lid, and the model core are 3d printed. The silicone rubber mold has an A30 durometer. Beeswax with a melting point of 63 °C is heated up to 95 °C for pouring into the rubber mold.

The titanium head constraint was water jetted out of a 0.9 mm thick highly corrosion-resistant grade 2 titanium plate. The center constraint was laser cut out of a 0.5 mm thick flexible acetal sheet. Both fabrication steps are depicted in Fig. 6.

In the final fabrication steps, two wax cores and both constraint layers are combined with the fish tail molds. The steps are depicted in Fig. 7.

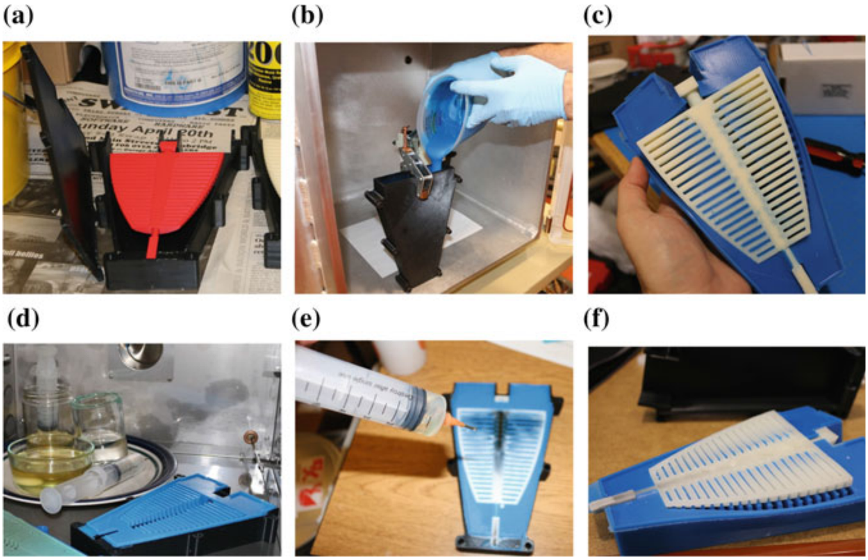

Fig. 5 Fabrication steps of the wax core. **a** 3d printed model core. **b** Create silicone mold. **c** Release model core. **d** Heating wax and mold. **e** Pour wax with syringe. **f** Demolding of wax core

Fig. 6 Laser cut center constraint layer and water jet head constraint

The tail consists of A15 durometer silicone rubber mixed with low density crush resistant glass bubbles to achieve a mixed density just below the density of water. The mixing ratio, n_b, between the bubble mass, m_b, and the silicone rubber mass, m_s, is: $n_b = \frac{m_b}{m_s} = (1 - \frac{\rho_d}{\rho_s})/(\frac{\rho_d}{\rho_b} - 1)$, where ρ_b stands for the density of the glass bubbles, ρ_s stands for the density of the silicone rubber, and ρ_d stands for the desired mixed density. The density of the used silicone rubber is $\rho_s = 1.18\,\text{g/cm}^3$ and the density of the glass bubbles is $\rho_b = 0.125\,\text{g/cm}^3$. In order to make the fish tail slightly lighter than water, a desired mixed density of $\rho_d = 0.991\,\text{g/cm}^3$ with a mixing ratio of $n_b = 2.3\,\%$ is used. This mixing step is important for achieving overall neutral buoyancy of the robotic fish. Otherwise, the weight of the fish tail has to be compensated with thick styrofoam flotation attachments around the center of the fish, which introduces undesired drag.

The nose of the fish is a waterproof housing for the microcontroller, motor driver, and wireless communication electronics. The housing is 3D printed and waterproofed

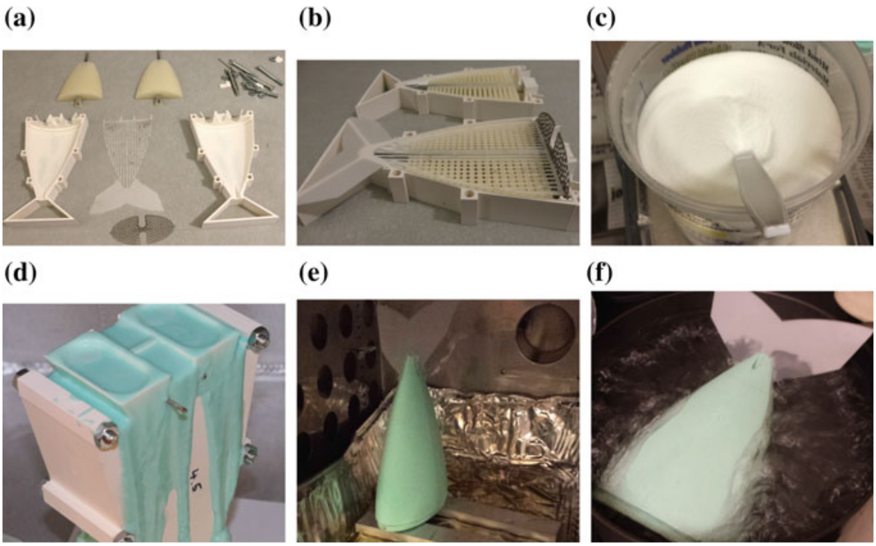

Fig. 7 Final fabrication steps of the silicone rubber fish tail. **a** Individual parts of tail mold assembly. **b** Create silicone mold. **c** Release model core. **d** Heating wax and mold. **e** Pour wax with syringe. **f** Demolding of wax core

by brush-coating it with a polyurethane paint and subsequent degassing [25]. Behind the nose is the dive plane assembly, consisting of two individually controllable dive plane units. Each unit consists of a dive plane, which is directly mounted onto the lever arm of a waterproof servo motor. The dive plane assembly is mounted to the end of the brushed DC motor of the gear pump. The motor and gear pump unit is directly attached to the soft fish tail. Underneath the gear pump motor sits a lithium polymer battery to power all components.

Each actuator has a removable plug at the caudal fin: the initial dive is started with plugs removed so water can fill the actuation chambers by running the self-priming gear pump at a low frequency for a short duration. After all air has been removed, the plugs are inserted to seal the chambers.

The 1.65 kg mass of the complete assembly was slightly adjusted to make it almost neutrally buoyant using foam attachments and additional weights placed outside and inside the 3D printed center hull of the fish. The fish has the dimensions: $0.45\,\text{m} \times 0.19\,\text{m} \times 0.13\,\text{m}$.

The fish receives 72 MHz wireless communication commands to move forward, move up and down, or turn left and right. The on-board micro-controller translates these high-level commands into the control law for the tail actuation and the angular positions of the dive planes.

The assembled fish with and without outer hulls is shown in Fig. 8.

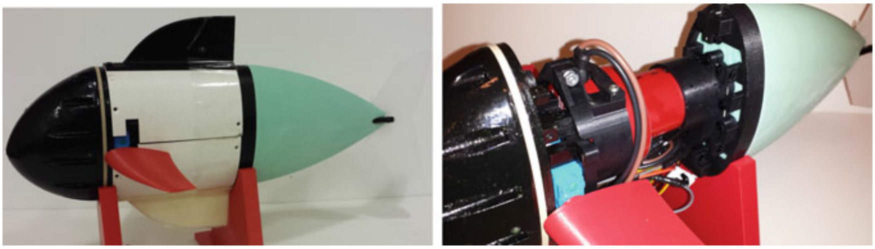

Fig. 8 Fully assembled soft robotic fish with and without outer hulls

4 Experiments

The goal of the experiments is to show the capabilities of the soft robotic fish in continuous forward swimming and pitch control, using a single battery loading. Additionally, yaw control was demonstrated in the pool experiments.

4.1 Fish Tank Experiments

The fish swam in a tank of a length of 1.22 m in a straight, horizontal line from wall to wall and repeated this 25 times. It was manually placed back to the start after each completion of one lap.

For an average horizontal distance of 0.74 m, the horizontal swimming speed was 0.10 m/s, which is equivalent to 0.15 body lengths per second. One repetition of the horizontal forward swimming experiment is shown in Fig. 9.

To test the pitch control, the fish's submergence was adjusted as it moved forward over the span of the tank by setting the pitch angle of the dive planes to $\frac{\pi}{4}$ rad. For 13 repetitions of this experiment, the average diving speed was 0.015 m/s over an average vertical distance of 0.13 m. The horizontal swimming speed was 0.08 m/s

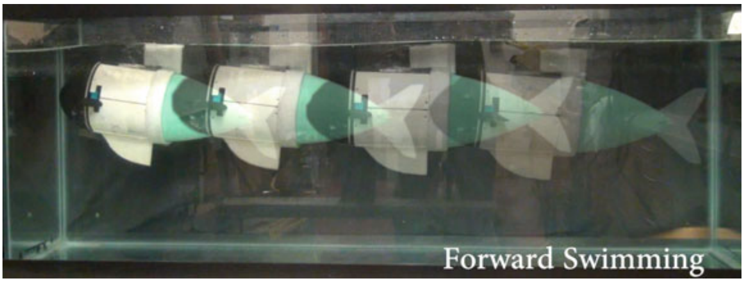

Fig. 9 Fish tank experiment: forward swimming

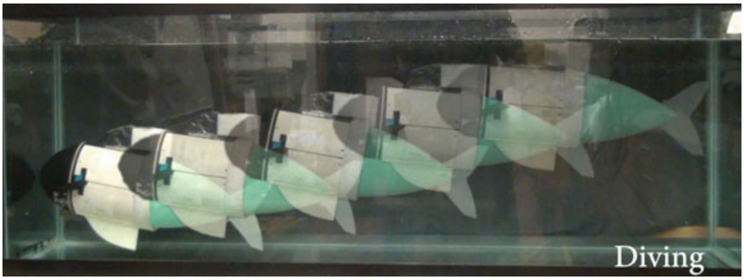

Fig. 10 Fish tank experiment: diving

over an average horizontal distance of 0.74 m. One repetition of the diving experiment is shown in Fig. 10.

After 35 min of continuous wireless underwater operation, the 1.3 Ah lithium polymer battery was almost depleted. This corresponded to 52 repeated runs through the tank, resulting in a total distance of approximately 40 m.

4.2 Pool Experiments

In a 13.25 m × 7 m × 1.12 m pool, the maximum horizontal swimming speed was 0.23 body lengths per second. One trial of the horizontal forward swimming experiment in the pool is shown in Fig. 9. The figure shows overlaid fish's poses for every time it had moved for one full body length.

To test the pitch control, the fish's submergence was adjusted as it moved near the side wall of the pool. The pitch angle of the dive planes was set to approximately $\frac{\pi}{4}$ rad. One trial of the diving experiment in the pool is shown in Fig. 11b.

The heading or yaw control was also tested. The fish was able to turn in the pool, as can be seen in Fig. 11c.

After about 40 min of continuous operation in the pool and swimming an accumulative distance of approximately 130 m, the 1.3 Ah lithium polymer battery was almost depleted.

5 Main Experimental Insights

The approach proposed in this work for creating an autonomous soft-bodied robotic fish resulted in a robot that demonstrated prolonged and consistent underwater operation. While most soft robots are pneumatically powered, it was shown that hydraulic power increases the capabilities for a given range of applications. For example, when high frequency change of actuation direction is needed, exemplified by the flapping

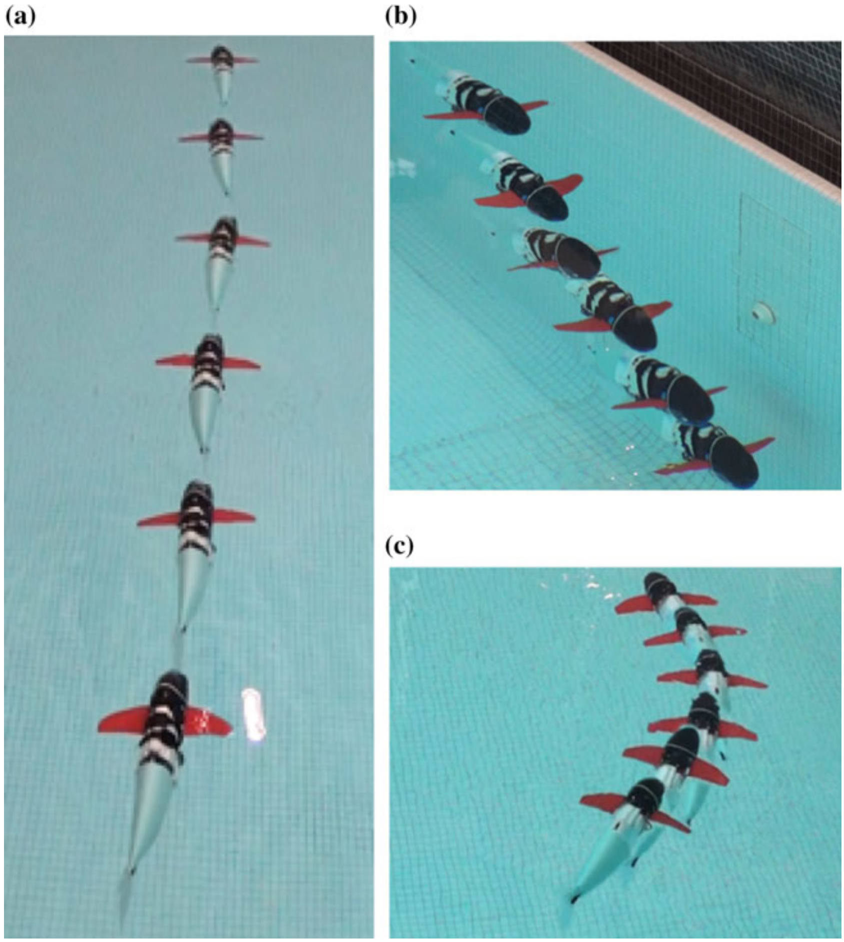

Fig. 11 Pool experiments demonstrating locomotion capabilities. **a** Forward swimming. **b** Turning

foil, or prolonged actuation of an autonomous soft robot is required. Hydraulic actuation allows for a higher force as shown by the overcoming of hydrodynamic resistance used for the fish-like locomotion [26]. The presented prototype is a step towards creating a closed-loop controlled biomimetic robotic fish which is inherently soft, performs continuous body deformations from nose to tail, and allows for safe interaction with other living beings. Based on the experimental results, the novel actuation system of the robot prototype will influence future work in the field, both in terms of fish robots and soft robots in general.

References

1. Albu-Schaffer, A., Eiberger, O., Grebenstein, M., Haddadin, S., Ott, C., Wimbock, T., Wolf, S., Hirzinger, G.: Soft robotics. IEEE Robot. Autom. Mag. **15**(3), 20–30 (2008)
2. Correll, N., Onal, C.D., Liang, H., Schoenfeld, E., Rus, D.: Soft autonomous materials - using active elasticity and embedded distributed computation. In: 12th International Symposium on Experimental Robotics (ISER), New Delhi, India (2010)
3. Onal, C.D., Chen, X., Whitesides, G.M., Rus, D.: Soft mobile robots with on-board chemical pressure generation. In: International Symposium on Robotics Research (ISRR) (2011)
4. Marchese, A.D., Onal, C.D., Rus, D.: Soft robot actuators using energy-efficient valves controlled by electropermanent magnets. In: 2011 IEEE/RSJ International Conference on Intelligent Robots and Systems (IROS), pp. 756–761. IEEE (2011)
5. Marchese, A.D., Onal, C.D., Rus, D.: Autonomous soft robotic fish capable of escape maneuvers using fluidic elastomer actuators. Soft Robot. **1**(1) (2014)
6. Barrett, D.S.: Propulsive efficiency of Robotuna. Ph.D. thesis, Massachusetts Institute of Technology (1988)
7. Triantafyllou, M.S., Triantafyllou, G.S.: An efficient swimming machine. Sci. Am. **272**(3), 64–71 (1995)
8. Zhong, Y., Chong, C., Zhou, C., Seet, G.G., Low, K.: Performance predict model for a body and caudal fin (bcf) biomimetics fish robot. In: International Conference on Advanced Intelligent Mechatronics, IEEE/ASME, pp. 1230–1235 (2009)
9. Liu, J., Hu, H.: Biological inspiration: from carangiform fish to multi-joint robotic fish. J. Bionic Eng. **7**(1), 35–48 (2010)
10. Wen, L., Wang, T., Wu, G., Liang, J.: Hydrodynamic investigation of a self-propelled robotic fish based on a force-feedback control method. Bioinspir. Biomim. **7**(3), 036012 (2012)
11. Rossi, C., Colorado, J., Coral, W., Barrientos, A.: Bending continuous structures with smas: a novel robotic fish design. Bioinspir. Biomim. **6**(4), 045005 (2011)
12. Trivedi, D., Rahn, C.D., Kier, W.M., Walker, I.D.: Soft robotics: biological inspiration, state of the art, and future research. Appl. Bionics Biomech. **5**(3), 99–117 (2008)
13. Laschi, C., Cianchetti, M., Mazzolai, B., Margheri, L., Follador, M., Dario, P.: Soft robot arm inspired by the octopus. Adv. Robot. **26**(7), 709–727 (2012)
14. El Daou, H., Salumae, T., Ristolainen, A., Toming, G., Listak, M., Kruusmaa, M.: A biomimetic design and control of a fish-like robot using compliant structures. In: 15th International Conference on Advanced Robotics (ICRA), pp. 563–568. IEEE (2011)
15. El Daou, H., Salumae, T., Toming, G., Kruusmaa, M.: A bio-inspired compliant robotic fish: Design and experiments. In: IEEE International Conference on Robotics and Automation (ICRA), pp. 5340–5345. IEEE (2012)
16. Valdivia y Alvarado, P., Youcef-Toumi, K.: Design of machines with compliant bodies for biomimetic locomotion in liquid environments. ASME J. Dyn. Syst. Meas. Control **128**, 3–13 (2006)
17. Long, J.H., Koob, T., Schaefer, J., Summers, A., Bantilan, K., Grotmol, S., Porter, M.: Inspired by sharks: a biomimetic skeleton for the flapping, propulsive tail of an aquatic robot. Mar. Technol. Soc. J. **45**(4), 119–129 (2011)
18. Long, J.H., Krenitsky, N.M., Roberts, S.F., Hirokawa, J., de Leeuw, J., Porter, M.E.: Testing biomimetic structures in bioinspired robots: how vertebrae control the stiffness of the body and the behavior of fish-like swimmers. Integr. Comp. Biol. **51**(1), 158–175 (2011)
19. Shen, Q., Wang, T., Liang, J., Wen, L.: Hydrodynamic performance of a biomimetic robotic swimmer actuated by ionic polymer-metal composite. Smart Mater. Struct. **22**(7), 075035 (2013)
20. Suzumori, K., Endo, S., Kanda, T., Kato, N., Suzuki, H.: A bending pneumatic rubber actuator realizing soft-bodied manta swimming robot. In: International Conference on Robotics and Automation, pp. 4975–4980. IEEE (2007)
21. Festo: Airacuda. http://www.festo.com/cms/en_corp/9761.htm (2006). Accessed 24 May 2014

22. Lauder, G.V., Flammang, B., Alben, S.: Passive robotic models of propulsion by the bodies and caudal fins of fish. Integr. Comp. Biol. **52**(5), 576–587 (2012)
23. Alben, S., Witt, C., Baker, T.V., Anderson, E., Lauder, G.V.: Dynamics of freely swimming flexible foils. Phys. Fluids (1994-present) **24**(5) 051901 (2012)
24. Karassik, I.J., Messina, J.P., Cooper, P., Heald, C.C.: Pump Handbook, vol. 4. McGraw-Hill, New York (2008)
25. Mireles, J., Adame, A., Espalin, D., Medina, F., Winker, R., Hoppe, T., Zinniel, B., Wicker, R.: Analysis of sealing methods for fdm-fabricated parts. Technical Report, W.M. Keck Center for 3D Innovation. The University of Texas, El Paso (2011)
26. Drucker, E.G., Lauder, G.V.: Locomotor forces on a swimming fish: three-dimensional vortex wake dynamics quantified using digital particle image velocimetry. J. Exp. Biol. **202**(18), 2393–2412 (1999)